PHYSICAL REVIEW C **86**, 031301(R) (2012)

Corrections to nuclear energies and radii in finite oscillator spaces

R. J. Furnstahl,[1] G. Hagen,[2,3] and T. Papenbrock[2,3]
[1]*Department of Physics, The Ohio State University, Columbus, Ohio 43210, USA*
[2]*Physics Division, Oak Ridge National Laboratory, Oak Ridge, Tennessee 37831, USA*
[3]*Department of Physics and Astronomy, University of Tennessee, Knoxville, Tennessee 37996, USA*
(Received 27 July 2012; published 5 September 2012)

We derive corrections to the ground-state energies and radii of atomic nuclei that result from the limitations of finite oscillator spaces.

DOI: 10.1103/PhysRevC.86.031301 PACS number(s): 21.60.−n, 21.10.Dr, 21.10.Gv, 03.65.Ge

Introduction. The oscillator basis is widely used in nuclear structure computations because it allows the practitioner to exploit and implement all symmetries of the nuclear many-body problem, and because its localized nature corresponds well to the structure of the self-bound atomic nucleus. After all, the nuclear shell model is based on the harmonic oscillator with a strong spin-orbit splitting [1]. Several computational implementations of *ab initio* methods [2,3] and nuclear density functional theory [4] essentially start from the oscillator basis. Basic observables sought in such computations include the binding energies and radii. Ideally, the computed observables should be independent of the parameters of the employed oscillator space, i.e., the maximum number of oscillator quanta N and the frequency Ω of the oscillator wave functions. This ideal is often difficult to reach in practice, so various empirical extrapolation schemes [5–9] have been applied, but all lack a firm theoretical foundation.

The proper accounting for corrections to nuclear energies and radii that arise in finite oscillator spaces is an important problem for several reasons. First, a theoretical foundation of such corrections would enable the practitioner to extrapolate reliably from smaller model spaces and thus extend the reach of some computational methods. This is particularly important for weakly bound nuclei where the Gaussian falloff of the oscillator basis can capture a halo state often only in unachievable large model spaces [6]. Second, uncertainty quantification of results—standard in experimental research—is increasingly taking place in nuclear structure theory [10]. Here, the quantification of theoretical uncertainties due to the nuclear interaction is possible for interactions from effective field theory (EFT), but the robust quantification of errors due to finite oscillator spaces is lacking. Finally, important steps toward an harmonic-oscillator-based EFT for the nuclear shell model have been made recently [11–13]. Such a theory should also control and exploit the limitations of the finite model space.

In this Rapid Communication, we derive corrections of nuclear energies and radii that are due to finite oscillator spaces. We build on the insights of Coon *et al*. [11], who focus on the infrared and ultraviolet cutoffs induced by a truncated basis. Our derivations are based on simple arguments and verified in a one-dimensional model. We apply the results to ^{16}O and demonstrate that the theoretical corrections agree well with the numerical data. Calculations for the ^{6}He ground-state energy and neutron radius show that predictions are feasible even for halo nuclei.

Theoretical derivation. For a particle in a box with periodic boundary conditions, Lüscher derived the corrections to bound states due to the finite size of the box [14]. Our derivation is analogous, except that the size of the box is now given in terms of the spatial extension of the oscillator basis and we deal essentially with Dirichlet boundary conditions [15]. Let us consider a model space of oscillator wave functions with maximum oscillator energy $E = \hbar\Omega(N + 3/2)$. In practice, one has to choose $\hbar\Omega$ and N such that the momentum cutoff λ of the employed interaction is smaller than the ultraviolet (UV) momentum,

$$\Lambda_{\mathrm{UV}} \equiv \sqrt{2(N + 3/2)}\hbar/b, \tag{1}$$

and that the radius r of the nucleus is smaller than the radial extent,

$$L_0 \equiv \sqrt{2(N + 3/2)}b, \tag{2}$$

of the employed oscillator space. Here, $b \equiv \sqrt{\hbar/(m\Omega)}$ is the oscillator length of our basis, and m denotes the nucleon mass. Equations (1) and (2) are indeed the maximum momentum and displacement, respectively, of a particle in a harmonic oscillator at energy $E = \hbar\Omega(N + 3/2)$. They differ from previous scaling relations [16,17] by factors of $\sqrt{2}$.

In practice, satisfying the UV condition $\lambda < \Lambda_{\mathrm{UV}}$ and the infrared (IR) condition $r < L_0$ does not guarantee converged nuclear structure results in the oscillator basis because the momentum cutoff λ is usually not sharp, and the nuclear wave function extends beyond the nuclear radius r. However, nuclear interactions from chiral EFT and from renormalization group transformations exhibit a super-Gaussian falloff in momentum space, whereas the nuclear wave function only falls off exponentially in coordinate space. Thus, once $\lambda < \Lambda_{\mathrm{UV}}$ holds, the UV convergence in momentum space will be rapid, and one is dominated by corrections from the slower falloff in coordinate space. Practitioners of nuclear structure computations know this very well (see, e.g., Fig. 6 below): When energies are plotted as a function of $\hbar\Omega$, the minimum initially shifts toward larger values of $\hbar\Omega$ as N is increased. However, once UV convergence has been reached, further increasing N shifts the minimum back to lower values of $\hbar\Omega$ to capture the coordinate-space tail of the wave function. In what follows, we will assume UV convergence and compute the correction from incomplete IR convergence.

The finite extent of the oscillator basis up to a radius L in coordinate space essentially requires the wave function to

 ©2012 American Physical Society

vanish at $r \approx L$. The maximum radius L_0 from Eq. (2) is only a leading-order (or asymptotically valid) estimate because the oscillator wave function decays rapidly beyond the classical turning point. An improved estimate for L using the intercept of the tangent at $r = L_0$ is [18]

$$L \approx L_0 + 0.54437\, b\, (L_0/b)^{-1/3}, \tag{3}$$

which we use with the analogous expression for $\Lambda_{\rm UV}$ in numerical examples below. For our derivation of IR corrections, we adapt the discussion in Ref. [19]. Given a boundary condition at $r = L$ beyond the range of the nuclear potential, we write the energy compared to that for $L = \infty$ as

$$E_L = E_\infty + \Delta E_L, \tag{4}$$

and we seek an estimate for ΔE_L, which is assumed to be small.

Let $u_E(r)$ be the radial solution with regular boundary condition at the origin and energy E. We denote the particular solutions $u_{E_L}(r) \equiv u_L(r)$ and $u_{E_\infty}(r) \equiv u_\infty(r)$. Then the linear energy approximation is (for $r \leqslant L$) [19]

$$u_L(r) \approx u_\infty(r) + \Delta E_L \left.\frac{du_E(r)}{dE}\right|_{E_\infty}, \tag{5}$$

assuming a smooth expansion of u_E about $E = E_\infty$ at fixed r. Evaluating Eq. (5) at $r = L$ with the boundary condition $u_L(L) = 0$, we find

$$\Delta E_L \approx -u_\infty(L)\left(\left.\frac{du_E(L)}{dE}\right|_{E_\infty}\right)^{-1}, \tag{6}$$

which is the estimate we seek. For general E, the asymptotic form of the radial wave function for r greater than the range R of the potential is

$$u_E(r) \xrightarrow{r\gg R} A_E(e^{-k_E r} + \alpha_E e^{+k_E r}), \tag{7}$$

with the known case $u_\infty(r) \xrightarrow{r\gg R} A_\infty e^{-k_\infty r}$ for $E = E_\infty$. Here, k_∞ is determined by the nucleon separation energy:

$$S = \frac{\hbar^2 k_\infty^2}{2m}. \tag{8}$$

We take the derivative of Eq. (7) with respect to energy, evaluate at $E = E_\infty$, using $\alpha_{E_\infty} = 0$ and $dk_E/dE = -m/(\hbar^2 k_E)$, to find

$$\left.\frac{du_E(r)}{dE}\right|_{E_\infty} = +A_\infty \left.\frac{d\alpha_E}{dE}\right|_{E_\infty} e^{+k_\infty r} + \mathcal{O}(e^{-k_\infty r}). \tag{9}$$

Substituting Eq. (9) at $r = L$ into Eq. (6), we obtain

$$\Delta E_L \approx -\left[\left.\frac{d\alpha_E}{dE}\right|_{E_\infty}\right]^{-1} e^{-2k_\infty L} + \mathcal{O}(e^{-4k_\infty L}). \tag{10}$$

The prefactor in the square brackets depends on details of the interaction (but not on L) and will be fit to numerical data when Eq. (10) is used together with Eq. (4). Thus, the main result is

$$E_L = E_\infty + a_0 e^{-2k_\infty L}, \tag{11}$$

and in practical applications one can treat E_∞, a_0, and k_∞ (in cases where the separation energy is not known) as fit parameters. Note that our Eq. (11) explains the exponential decay observed empirically in Ref. [11]. In contrast to the Lüscher result in which the energy is always lowered by periodic images of the potential [14], the energy from Eq. (11) is always increased by the shift of a node from $r = \infty$ to $r = L$, consistent with the variational nature of the truncated basis expansion.

Let us next turn to radii. It is convenient to express the radius squared as the infinite-model-space result plus a correction term

$$\langle r^2\rangle_L = \langle r^2\rangle_\infty + \Delta\langle r^2\rangle_L, \tag{12}$$

where

$$\Delta\langle r^2\rangle_L = \frac{\int_0^L |u_L(r)|^2\, r^2\, dr}{\int_0^L |u_L(r)|^2\, dr} - \frac{\int_0^\infty |u_\infty(r)|^2\, r^2\, dr}{\int_0^\infty |u_\infty(r)|^2\, dr}. \tag{13}$$

Because the dependence on L of $u_L(r)$ in Eq.(5) is confined to ΔE_L, when u_L is substituted into Eq. (13) the L dependence of each separate integrand comes entirely from the upper integration limit. Therefore, we can use the asymptotic expressions $u_\infty(r) \longrightarrow A_\infty e^{-k_\infty r}$ and

$$\left.\frac{du_E(r)}{dE}\right|_{E_\infty} \approx -\frac{A_\infty}{\Delta E_L} e^{-2k_\infty L} e^{+k_\infty r} \tag{14}$$

to identify the leading-order expression $\Delta\langle r^2\rangle_L \propto \langle r^2\rangle_\infty (2k_\infty L)^3 e^{-2k_\infty L}$. [Note that any L-independent terms are guaranteed to cancel by the definition Eq. (13).] The next-to-leading-order expression scales as $(2k_\infty L)\exp(-2k_\infty L)$ because the condition $u_L(L) = 0$ ensures there is no quadratic term in $2k_\infty L$. Thus, the L dependence of the squared radius is (with $\beta \equiv 2k_\infty L$) [18]

$$\langle r^2\rangle_L \approx \langle r^2\rangle_\infty [1 - (c_0\beta^3 + c_1\beta)e^{-\beta}]\,. \tag{15}$$

Here, $\langle r^2\rangle_\infty$, c_0, and c_1 are fit parameters while k_∞ should be determined in fitting the energy Eq. (11). The approximation Eq. (15) is valid in the asymptotic regime $\beta \gg 1$. In practice, one needs $\beta \gtrsim 3$ because the leading-order correction has its maximum at $\beta = 3$, and the next-to-leading order corrections is approximately suppressed by one order of magnitude for $\beta \gtrsim 3$ (with c_0 and c_1 of order unity).

Equations (11) and (15) are the main results of this Rapid Communication. A few comments are in order before we turn to applications of these results. Note that we derived these results in the laboratory system. For the nuclear A-body problem, we could also have exploited the separation of the center-of-mass coordinate in the oscillator basis and followed a similar derivation for the Ath particle with respect to the center of mass of the remaining $(A-1)$ particles. This would rescale L and the momentum of the Ath particle accordingly, but the final results are unchanged when re-expressed in laboratory coordinates. In situations where the relevant threshold involves two clusters of nucleons (multiple clusters of nucleons), a similar reasoning applies to the relative coordinate between the two clusters (the hyperradius). Due to these comments, and in light of the approximations involved in defining L and the corrections to the energy and radius, in actual fits to numerical results one might want to treat k_∞ as a fit parameter even

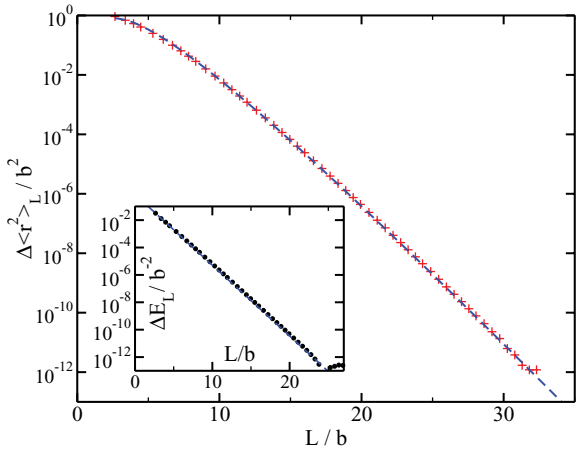

FIG. 1. (Color online) Finite-basis-size correction of the squared radius (crosses) compared to Eq. (15) (dashed line) for a toy model. The squared radius is $r_\infty^2/b^2 \approx 1.736$, and $k_\infty b \approx 0.595$. Inset: Finite-basis-size correction of the energy (data points) compared to Eq. (10) (dashed line).

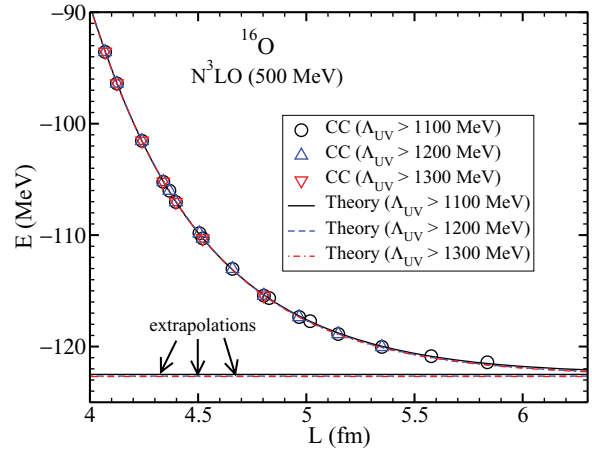

FIG. 2. (Color online) Open symbols: Ground-state energy of ^{16}O as a function of L. Lines: Fits to Eq. (11) yield $E_\infty \approx -122.6$ MeV and $k_\infty \approx 0.95\,\mathrm{fm}^{-1}$. Λ_{UV} from Eq. (1).

when the corresponding separation energy or breakup energy is known.

Applications. As a first check, we consider a toy model in one dimension with the Hamiltonian $H = p^2/2 - v_0 \exp(-x^2)$. Here, x is given in units of the oscillator length b. In one dimension, the constant $3/2$ in Eqs. (1) and (2) has to be replaced by $1/2$. We compute the ground-state energy and the squared radius for $v_0 = 0.5$ in large oscillator spaces to obtain fully converged results for the ground-state energy and the radius. In this simple case, the ground-state energy is given in terms of the separation energy Eq. (8) as $E_\infty = -S$. Figure 1 shows the correction $\Delta\langle r^2\rangle$ as a function of L. The dashed line results from a leading-order fit to Eq. (15), and the agreement between numerical data and the theoretical prediction extends over ten orders of magnitude. The inset shows that the L-dependent energy correction also agrees with the prediction Eq. (11).

Let us turn to the nuclear many-body problem. We employ the nucleon-nucleon interaction from chiral EFT by Entem and Machleidt [20] and compute the ground-state energy and radius of the nucleus ^{16}O with the coupled-cluster method in its singles and doubles approximation with triples corrections [16,21]. In our computation of energies and radii we used the intrinsic Hamiltonian and intrinsic radius squared operator in model spaces with frequencies $42 \leqslant \hbar\Omega/\mathrm{MeV} \leqslant 76$ and with $N = 12, 14$. To ensure that the computed results are practically UV converged, we only use those oscillator spaces for which Λ_{UV} is sufficiently large. Figure 2 shows the results for the ground-state energy as a function of L. The circles, up triangles, and down triangles denote points with $\Lambda_{UV} > 1100$ MeV, $\Lambda_{UV} > 1200$ MeV, and $\Lambda_{UV} > 1300$ MeV, respectively. The points all fall on a line because UV convergence has practically been achieved. Thus, we can apply our theory. The lines show fits to Eq. (11) with fit parameters E_∞, a_0, and k_∞. Note that the result $E_\infty \approx -122.6$ MeV of the fit depends very weakly on Λ_{UV}, the difference being about 0.2 MeV. In the fits, we obtain $k_\infty \approx 0.95\,\mathrm{fm}^{-1}$, and this agrees well with the decay of the $p_{1/2}$ orbital that contributes to the density [22].

Next we consider the radius. We use Eq. (15), including the next-to-leading order correction, and fit the parameters $\langle r^2\rangle_\infty$, c_0, and c_1 to data, with k_∞ taken from the fit of the ground-state energy. The result is shown in Fig. 3. The circles, up triangles, and down triangles denote points with $\Lambda_{UV} > 1100$ MeV, $\Lambda_{UV} > 1200$ MeV, and $\Lambda_{UV} > 1300$ MeV, respectively. The lines show the corresponding fits and asymptotes, and the extrapolated radius is $r \approx 2.34$ fm. It is particularly satisfying that the extrapolation also works well for the few data points with $\Lambda_{UV} > 1300$ MeV.

We also consider the challenging case of a halo nucleus. The isotope ^{6}He is only bound by about 0.97 MeV with respect to ^{4}He and thus exhibits a two-neutron halo. Note that ^{5}He is not a bound nucleus and that the neutron separation energy of ^{6}He is about 1.86 MeV. As a consequence of the weak binding, the matter radius of ^{6}He is unusually large (about 2.4 fm compared to 1.5 fm for ^{4}He) [23–25]. We address this

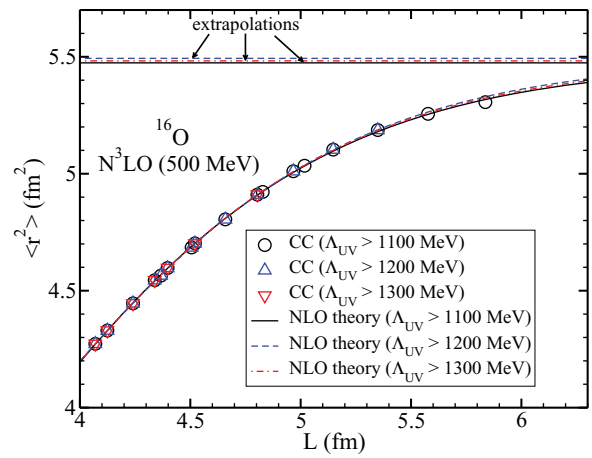

FIG. 3. (Color online) Open symbols: Squared radius as a function of L for ^{16}O. Lines: Fits of Eq. (15) with k_∞ fixed from the energy fit. Λ_{UV} from Eq. (1).

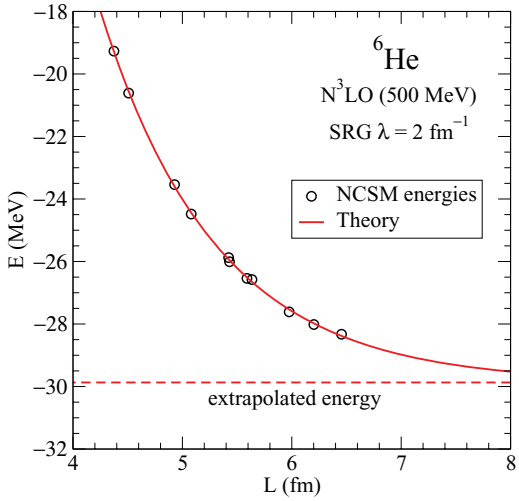

FIG. 4. (Color online) Circles: NCSM ground-state energies of the halo nucleus ^{6}He from Ref. [6]. Full line: Fit of Eq. (11) yields $E_\infty \approx -29.87$ MeV (dashed line) and $\hbar k_\infty \approx 93$ MeV.

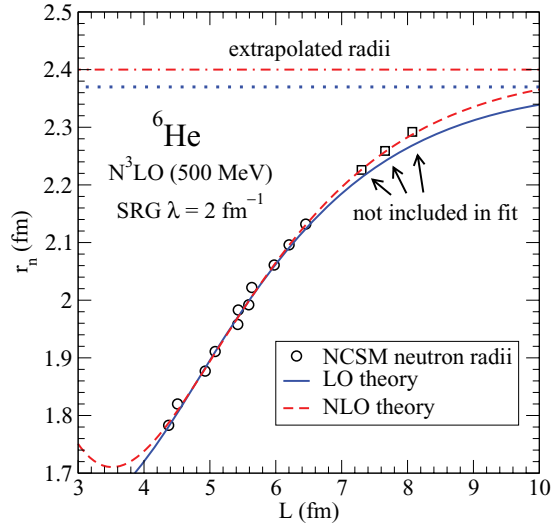

FIG. 5. (Color online) Circles and squares: NCSM neutron radii of ^{6}He. Lines: Fits of Eq. (15) to circles with k_∞ fixed from energy fit yield a radius of 2.37 fm at LO and 2.40 fm at NLO.

challenge by applying the finite-basis-size corrections to the energy Eq. (11) and neutron radius Eq. (15).

Our test case uses no-core shell model (NCSM) results [6] obtained for a chiral EFT nucleon-nucleon interaction that was softened via a similarity renormalization group (SRG) transformation [26] with a parameter $\lambda = 2.0$ fm^{-1}. Figure 4 shows the fit of the ground-state energy for model spaces with $\Lambda_{\rm UV} > 660$ MeV and $\hbar\Omega \geqslant 24$ MeV (which ensures a small UV correction). The fit yields $E_\infty \approx -29.87$ MeV, and the computed two-neutron separation energy is about 0.95 MeV. Thus, both energies are in good agreement with experiment (despite the absence of a three-body force). The fit also yields $\hbar k_\infty \approx 93$ MeV, but the interpretation of k_∞ in this case requires further study.

Now we can extrapolate the neutron radius of ^{6}He. The results of NCSM calculations are shown in Fig. 5. Without a knowledge of the finite-basis-size corrections, it would be impossible to make any reasonable prediction for the radius because of the apparent lack of convergence. Note, however, that we are in the UV-converged regime and $2k_\infty L > 3$ for the NCSM data points in Fig. 4. Thus, we should be able to apply our correction formula. The solid and dashed lines in Fig. 5 show the results for the radius based on a fit at leading order and next-to-leading order, respectively. At next-to-leading order we find $r \approx 2.40$ fm, and this prediction is in reasonable agreement with deductions from data [24]. Several additional points at large L not included in the fit are in good agreement with the extrapolation.

Our theoretical results have been derived under the assumption that UV convergence has been reached. It would also be useful to know finite-basis-size corrections in the opposite regime where IR convergence is established, for instance, through calculations in model spaces with sufficiently small $\hbar\Omega$. The remaining UV corrections would, of course, depend on the interaction at hand. We have not yet established a theoretical derivation but can resort to empirical findings for SRG-evolved nucleon-nucleon interactions from chiral EFT with an SRG parameter λ [6]. We plotted IR converged ground-state energies (computed at large values of $2k_\infty L$) for various light nuclei as a function of $\Lambda_{\rm UV}$ and found as in Refs. [11,12] that the empirical formula

$$E(\Lambda_{\rm UV}) = E_\infty + A_0 e^{-2(\frac{\Lambda_{\rm UV}}{\lambda})^2} \tag{16}$$

works quite well [18]. (In practice, we allow λ to be a fit parameter to optimize the fit.) This formula is consistent with an empirically successful ansatz used for individual $\hbar\Omega$ values (e.g., see Ref. [6]). However, Eq. (16) allows results with different $\hbar\Omega$ to be fit all at once.

If we combine the empirical UV formula and the theoretically founded IR formula assuming the corrections are approximately independent, then

$$E(\Lambda_{\rm UV}, L) \approx E_\infty + A_0 e^{-2\Lambda_{\rm UV}^2/A_1^2} + A_2 e^{-2k_\infty L}. \tag{17}$$

Note that this empirical formula contains exponentials with arguments proportional to N (from $\Lambda_{\rm UV}^2$) and $\sqrt{N}$ (from L), and thereby differs from usually employed extrapolations that are exponential in N. In Eq. (17), E_∞, A_0, A_1, A_2, and k_∞ are fit parameters that are determined from a simultaneous optimization to data at all $\hbar\Omega$, including in the intermediate region where both IR and UV corrections are significant. The resulting value $E_\infty \approx -29.84$ MeV from using all $N_{\rm max} =$ 6–10 points, which is in good agreement with the IR-only fit in Fig. 4, is plotted as a dashed red line in Fig. 6. The points connected by dashed lines are obtained by subtracting the corrections in Eq. (17) from the NCSM energies. Thus, a perfect fit would find all points lying on the line for E_∞. (Note: the $N_{\rm max}$ values in the figure are for *excitations* above the ground state [6], so $N = N_{\rm max} + 1$ for ^{6}He [11,18].) All corrected points included in the fit are close to the E_∞ line and even the corrected $N_{\rm max} = 4$ energies (which were not included in the fit) are only slightly overbound.

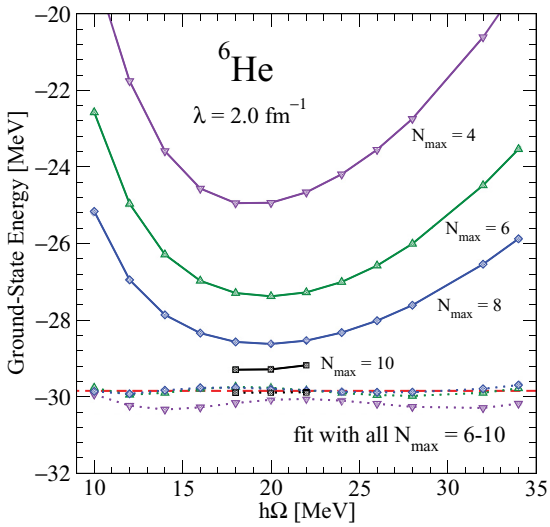

FIG. 6. (Color online) Data points connected by full lines: NCSM ground-state energies of ^{6}He. Red dashed line: Fit of Eq. (17) to NCSM data with $N_{\max} = 6$–10 yields $E_\infty \approx -29.84$ MeV. Data points connected with dotted line: Applying the correction of Eq. (17) to the NCSM data. ($N = N_{\max} + 1$).

In summary, we derived analytical results for the finite-basis-size corrections of nuclear radii and energies that are valid in oscillator spaces with converged ultraviolet physics. The computation of the corrections is robust and appears to be applicable to halo nuclei. In combination with an empirical formula for the ultraviolet correction for SRG-transformed interactions, consistent and much-improved extrapolations of ground-state energies are possible. The analytical results can be extended to other long-range observables that are sensitive to the tail of the nuclear density. A systematic study of the extrapolation procedure including an error analysis will be presented in a future work [18].

ACKNOWLEDGMENTS

We thank S. Bogner, S. Coon, K. Hebeler, U. Heinz, H. Hergert, M. Kruse, P. Maris, S. More, W. Nazarewicz, R. Perry, J. Vary, and K. Wendt for useful discussions. We also thank an anonymous referee for thoughtful comments. This work was supported in part by the National Science Foundation under Grant No. PHY–1002478 (The Ohio State University), and the Department of Energy under Grants No. DE-FG02-96ER40963 (University of Tennessee) and No. DEAC05-00OR22725 (Oak Ridge National Laboratory). This research used resources of the Leadership Computing Facility at the Oak Ridge National Laboratory.

[1] M. Mayer and J. H. D. Jensen, *Elementary Theory of Nuclear Shell Structure* (Wiley, New York, 1955).
[2] D. C. Zheng, B. R. Barrett, L. Jaqua, J. P. Vary, and R. J. McCarthy, Phys. Rev. C **48**, 1083 (1993).
[3] P. Navrátil, S. Quaglioni, I. Stetcu, and B. R. Barrett, J. Phys. G: Nucl. Part. Phys. **36**, 083101 (2009).
[4] J. Dobaczewski and J. Dudek, Comput. Phys. Commun. **102**, 183 (1997).
[5] G. Hagen, D. J. Dean, M. Hjorth-Jensen, T. Papenbrock, and A. Schwenk, Phys. Rev. C **76**, 044305 (2007).
[6] S. K. Bogner, R. J. Furnstahl, P. Maris, R. J. Perry, A. Schwenk, and J. P. Vary, Nucl. Phys. A **801**, 21 (2008).
[7] C. Forssén, J. P. Vary, E. Caurier, and P. Navrátil, Phys. Rev. C **77**, 024301 (2008).
[8] P. Maris, J. P. Vary, and A. M. Shirokov, Phys. Rev. C **79**, 014308 (2009).
[9] R. Roth, Phys. Rev. C **79**, 064324 (2009).
[10] S. K. Bogner, R. J. Furnstahl, and A. Schwenk, Prog. Part. Nucl. Phys. **65**, 94 (2010).
[11] S. A. Coon, M. I. Avetian, M. K. G. Kruse, U. van Kolck, P. Maris, and J. P. Vary, arXiv:1205.3230 (2012).
[12] W. C. Haxton and C.-L. Song, Phys. Rev. Lett. **84**, 5484 (2000); arXiv:nucl-th/9906082.
[13] I. Stetcu, B. R. Barrett, and U. van Kolck, Phys. Lett. B **653**, 358 (2007).
[14] M. Lüscher, Commun. Math. Phys. **104**, 177 (1986).
[15] D. Lee and M. Pine, Eur. Phys. J. A **47**, 41 (2011); M. Pine and D. Lee, arXiv:1206.6280 (2012).
[16] G. Hagen, T. Papenbrock, D. J. Dean, and M. Hjorth-Jensen, Phys. Rev. C **82**, 034330 (2010).
[17] E. D. Jurgenson, P. Navrátil, and R. J. Furnstahl, Phys. Rev. C **83**, 034301 (2011).
[18] R. J. Furnstahl, G. Hagen, and T. Papenbrock (in preparation).
[19] D. Djajaputra and B. R. Cooper, Eur. J. Phys. **21**, 261 (2000).
[20] D. R. Entem and R. Machleidt, Phys. Rev. C **68**, 041001 (2003).
[21] F. Coester, Nucl. Phys. **7**, 421 (1958); F. Coester and H. Kümmel, *ibid.* **17**, 477 (1960); J. Čížek, J. Chem. Phys. **45**, 4256 (1966); Adv. Chem. Phys. **14**, 35 (1969); H. Kümmel, K. H. Lührmann, and J. G. Zabolitzky, Phys. Rep. **36**, 1 (1978).
[22] D. Van Neck, L. Van Daele, Y. Dewulf, and M. Waroquier, Phys. Rev. C **56**, 1398 (1997).
[23] I. Tanihata, D. Hirata, T. Kobayashi, S. Shirnoura, K. Sugimoto, and H. Toki, Phys. Lett. B **289**, 261 (1992).
[24] G. D. Alkhazov *et al.*, Phys. Rev. Lett. **78**, 2313 (1997).
[25] O. A. Kiselev *et al.*, Eur. Phys. J. A **25**, 215 (2005).
[26] S. K. Bogner, R. J. Furnstahl, and R. J. Perry, Phys. Rev. C **75**, 061001 (2007).